SBAS-InSAR Analysis of ALOS-2 and Sentinel-1 SAR Data for Monitoring Land Subsidence in the East Azerbaijan Province of Iran

Fatemeh Sedghi, Sadra Karimzadeh *

Department of Remote Sensing and GIS, University of Tabriz, Iran – fatemeh.sedghi@tabrizu.ac.ir, sadra.karimzadeh@gmail.com
* Corresponding author

Keywords: ALOS-2, Sentinel-1, Land subsidence, SBAS InSAR, East Azerbaijan Province.

ABSTRACT

Iran, as a semi-arid and arid country, has faced significant challenges in water resource management in recent decades. The over-extraction of groundwater, driven by improper agricultural development, has significantly contributed to land subsidence. Therefore, identifying and quantifying ground subsidence in major plains is crucial for mitigating potential hazards. Recently, the Interferometric Synthetic Aperture Radar (InSAR) technique has been widely used to measure land surface deformations, providing accurate monitoring of ground movement with high spatial and temporal coverage. This study utilized time-series SBAS analysis with L-band (PALSAR-2) and C-band (Sentinel-1) SAR data to examine long-term ground displacements in East Azerbaijan Province. The results indicated significant subsidence in two major regions, the Tabriz and Shabestar plains. The cumulative vertical displacement in the study area from 2015 to 2023 reached -587.7 mm, with maximum subsidence rates of -73.67 mm/year based on ALOS-2 data. A comparison of SBAS results between L-band PALSAR-2 and C-band Sentinel-1 data showed a high level of agreement. For Sentinel-1, the cumulative vertical displacement from 2017 to 2023 was -374.7 mm, with maximum subsidence rates of -59.97 mm/year.

1. INTRODUCTION

Land subsidence, characterized by the gradual and continuous sinking or downward movement of the Earth's surface, is primarily driven by excessive groundwater withdrawal, underground construction loads, and geological processes like tectonic shifts and soil compaction (Zhang et al, 2024). This phenomenon can result in surface cracking, infrastructure damage, transportation disruptions, and severe risks to public safety and property (Yi et al, 2025). As a result, precise and timely monitoring and forecasting of land subsidence are crucial for ensuring sustainable urban development and strengthening infrastructure resilience.

Precise land subsidence monitoring has traditionally relied on leveling, GNSS, and laser scanning. However, these methods are costly, time-consuming, and have limited spatial coverage, making them unsuitable for large-scale, high-precision monitoring (Zhang et al, 2024). With advances in remote sensing, Synthetic Aperture Radar Interferometry (InSAR) has become a key method for monitoring land subsidence, landslides, and infrastructure stability. Techniques like Differential Interference Radar (D-InSAR), Small Baseline Subset InSAR (SBAS-InSAR), and Persistent Scatterer InSAR (PS-InSAR) offer continuous operation in all weather conditions, cloud penetration, wide-area coverage, and cost efficiency compared to traditional methods ((Yi et al, 2025) & (Ashraf et al, 2024)). Compared to D-InSAR and PS-InSAR, SBAS-InSAR utilizes spatially distributed coherence, providing higher coherence and reduced noise in time-series displacement analysis (Yi et al, 2025). It selectively receives signals from locations with stable scattering patterns, enhancing deformation accuracy. SBAS-InSAR is valuable for geodetic applications such as ground subsidence (Karimzadeh et al, 2024) & (Haghshenas Haghighi & Motagh, 2024)), landslides (Sorkhabi et al, 2023), mining activities (Ashraf et al, 2024), and earthquakes (Su et al, 2016). Studies show it delivers reliable results in areas with varied deformation characteristics (Ashraf et al, 2024). High-resolution SAR satellites such as TerraSAR-X and ALOS-2 have been operated to achieve accurate and long-term monitoring using InSAR. However, conventional methods relying on a single sensor face limitations, including high costs and restricted access to high-resolution imagery. In contrast, the multi-sensor InSAR approach overcomes these limitations, providing greater accuracy in detecting ground deformation ((Huang et al, 2024) &(Karimzadeh & Matsuoka, 2020)). Additionally, this method offers broader spatial and temporal coverage and enhances the stability of results (Huang et al, 2024).

In this study, we performed time-series SBAS analysis using L-band radar images from the ALOS-2 satellite (2015–2023) and C-band radar images from the Sentinel-1 satellite (2017–2023) to investigate long-term ground displacements in East Azerbaijan Province. By comparing multi-sensor results, this paper evaluates data consistency and reliability, providing a more detailed analysis of the impact of human activities on land subsidence.

2. MATERIALS & METHODS

2.1. Study Area

This study focuses on land subsidence in the East Azerbaijan Province of northwestern Iran. This region has experienced a growing demand for groundwater resources due to industrial development, population growth, and the expansion of agricultural activities (Karimzadeh & Matsuoka, 2020). Consequently, over-extraction of groundwater has led to a decline in groundwater levels, resulting in land subsidence. Additionally, rising temperatures and decreasing precipitation have led to a reduction in surface water resources in East Azerbaijan Province, further increasing dependence on groundwater (Andaryani et al, 2019). As groundwater levels continue to decline, the land subsidence rate in the region has been steadily increasing, posing serious risks to buildings and urban infrastructure (Karimzadeh & Matsuoka, 2020). Given these circumstances, accurate monitoring of land subsidence rates and identification of the spatiotemporal patterns and driving factors of land subsidence are essential for effective risk management and sustainable urban development in the region. Figure 1 illustrates the study area.

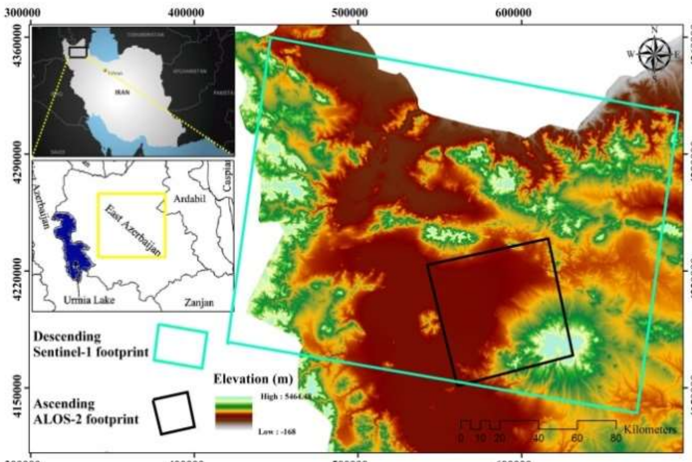

Figure 1. The study area is located in East Azerbaijan Province, Iran. The main map presents the region's digital elevation model (DEM). The black and cyan polygons show the footprints of ascending ALOS-2 and descending Sentinel-1 satellites, respectively.

2.2. Data

In this study, we utilized two sets of SAR data to monitor land deformation in the East Azerbaijan Province. The ALOS-2 L-band radar image, produced by the Japan Aerospace Exploration Agency (JAXA), spans from December 2015 to November 2023. Operating at a frequency of 1.2 GHz with a wavelength of 23.5 cm (Huang et al, 2024), ALOS-2 is currently the only operational L-band SAR satellite. Its longer wavelength makes it suitable for monitoring ground displacement in complex terrain and dense vegetation (Huang et al, 2024). In this study, we utilized 19 ALOS-2 images captured in ascending orbit, featuring HH polarization. The second dataset consists of C-band Sentinel-1 images collected from April 2017 to July 2023. We acquired these images with VV polarization in a descending orbit and they have a spatial resolution of approximately 5*20 meters. We utilized a total of 23 Sentinel-1 images for this analysis. A Digital Elevation Model (DEM) from the Shuttle Radar Topography Mission (SRTM) was used in the data processing. This DEM has a spatial resolution of 30 x 30 meters and a temporal accuracy of 1 arc-second. We utilized it to correct topographic effects and enhance the accuracy of land deformation measurements (Ashraf et al, 2024).

2.3. Method

The Small Baseline Subset InSAR (SBAS-InSAR) technique was first proposed by Berardino et al. in 2002 (Berardino et al, 2002). This method involves selecting M SAR images and flexibly combining them to ensure that each image forms at least one interferometric pair with another image. By establishing thresholds for temporal and spatial baselines, we exclude unsuitable image data. This reduction minimizes the impact of spatiotemporal decorrelation on monitoring results. Following this, differential interferometric processing is conducted on all image pairs using the small baseline combination method, resulting in N differential interferograms. We remove the flat-earth effect and topographic phase by using external Digital Elevation Model (DEM) data. The interferometric phase of the interferogram generated by two SAR images is expressed as follows:

$$\emptyset = \frac{4\pi}{\lambda}.(d_1 - d_2) + \Delta\emptyset_{top-error} + \emptyset_{atm} + \emptyset_{noi}$$

Where $\Delta\emptyset_{top-error}$ represents residual topographic phase error, $\emptyset_{atm}$ is an atmospheric delay, and $\emptyset_{noi}$ denotes noise. The SBAS-InSAR technique assumes that surface deformation follows a linear pattern. A linear model was developed to describe the deformation of the surface. The residual topographic phase error was estimated and removed using the Singular Value Decomposition (SVD) method. Additionally, atmospheric phase and nonlinear deformation were separated by applying a low-pass filter in the spatial domain and a high-pass filter in the temporal domain. The least squares method was then used to calculate the mean phase change rate and surface deformation. In this study, we set a spatial baseline threshold of 45% and a temporal baseline of 365 days. ALOS-2 image acquired on January 27, 2018, and Sentinel-1 image acquired on April 29 were selected as reference images. Figure 2 illustrate the generated image pairs and their corresponding baselines for the two sensors. We used external DEM data to assist interferometric processing. The Goldstein filter and the Delaunay Minimum Cost Flow (MCF) method were applied for phase unwrapping. After evaluating noise and analyzing phase information in the study area, we set the coherence threshold to 0.2. Orbital corrections and phase adjustments were then performed. Residual topographic phase error and atmospheric delay were estimated using two inversion processes, followed by geocoding to convert coordinates to the geographic reference system.

https://doi.org/10.5194/isprs-annals-X-4-W8-2025-701-2026 | © Author(s) 2026. CC BY 4.0 License.

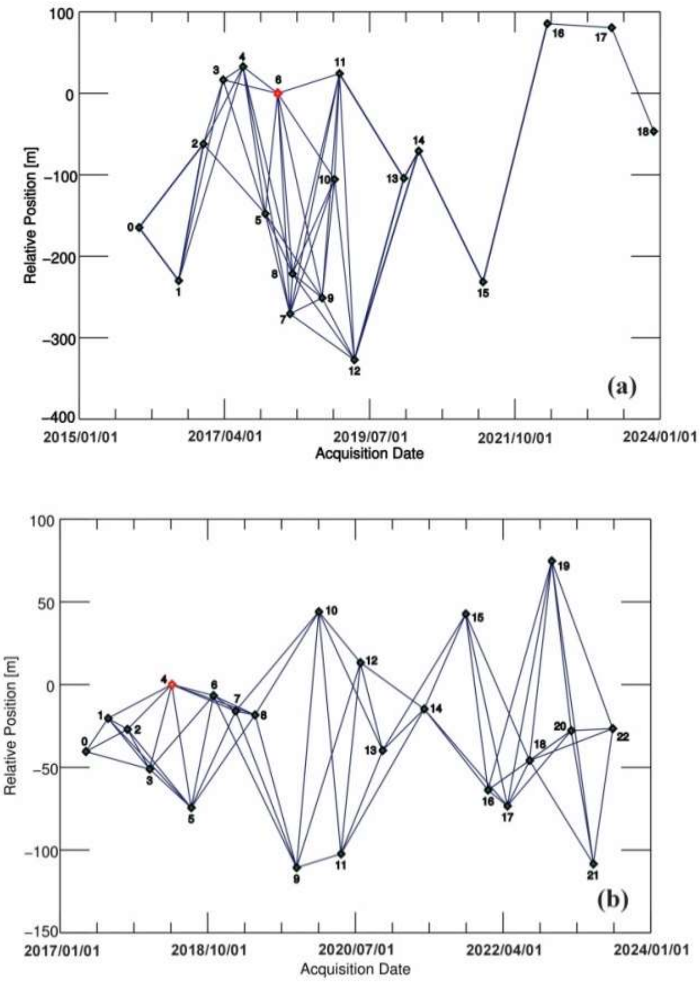

Figure 2. Image pairs and baselines generated by SBAS-InSAR: (a) ALOS-2 images and (b) Sentinel-1 images.

3. RESULTS

3.1. Coherence Changes

Figure 3 shows the spatiotemporal changes of the coherence histograms, analyzed using ALOS-2 images over eight time periods and Sentinel-1 images over six time periods, each spanning approximately one year. Despite the differences in the observational bands of the two satellites (L-band for ALOS-2 and C-band for Sentinel-1), the mean coherence values effectively reflect temporal changes in surface phenomena. The histogram shapes indicate that coherence stability over longer time intervals is higher for the L-band (ALOS-2), attributed to its greater penetration depth. In contrast, the C-band of Sentinel-1, due to its higher sensitivity to surface changes and vegetation cover, shows a noticeable decrease in the peak of the histogram, particularly in the 2019-2020 period. Although the overall behavior of the coherence maps is similar, the position of the histogram peak in the fifth period of ALOS-2 (2019-2020) differs from other periods (Figure 3-a). Additionally, the peak of the histogram in the third period of Sentinel-1 (2019-2020) is lower than in different periods (Figure 3-b). During this timeframe, heavy rainfall occurred across most parts of Iran from the beginning of spring, leading to flooding and waterlogging in many regions of the province. These events significantly impacted the signals recorded by the satellites. Furthermore, on November 8, 2019, an earthquake with a magnitude of 5.9 struck the Torkamanchay-Miyaneh area in the province. These events influenced the spatial and temporal variations observed in the coherence histograms.

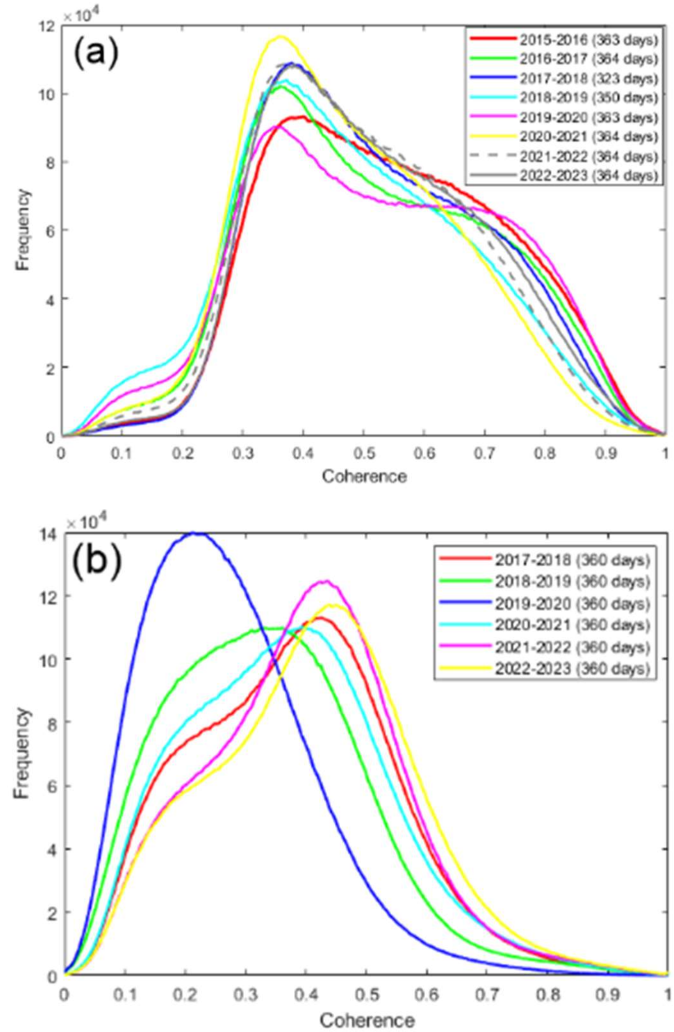

Figure 3. Coherence variation statistics for SAR pairs with ~1-year time spans: (a) ALOS-2, (b) Sentinel-1.

3.2. InSAR Displacements and time series

Figure 4 displays the comparative results of land subsidence rates in the East Azerbaijan Province, based on the SBAS InSAR

This contribution has been peer-reviewed. The double-blind peer-review was conducted on the basis of the full paper.
https://doi.org/10.5194/isprs-annals-X-4-W8-2025-701-2026

technique. The analysis uses two datasets: ALOS-2, covering 2015 to 2023, and Sentinel-1, covering 2017 to 2023. Both datasets exhibit a similar pattern of displacement rates throughout the region. These results indicate significant ground surface changes in the Tabriz and Shabestar plains, the most affected subsidence areas in this province. Previous studies have identified these two areas as subsidence hotspots ((Haghshenas Haghighi & Motagh, 2024) & (Karimzadeh & Matsuoka, 2020)). The maximum vertical subsidence rate is -73.66 mm/year for ALOS-2 and -59.97 mm/year for Sentinel-1. This difference could be attributed to several reasons. Firstly, the wavelength of ALOS-2 images is longer than that of Sentinel-1, which leads to differences in the sensitivity of the two datasets when detecting ground displacements. Additionally, ALOS-2 has a more extended observation period (2015-2023) compared to Sentinel-1 (2017-2023). This difference in observation duration may have resulted in ALOS-2 capturing more cumulative changes over time.

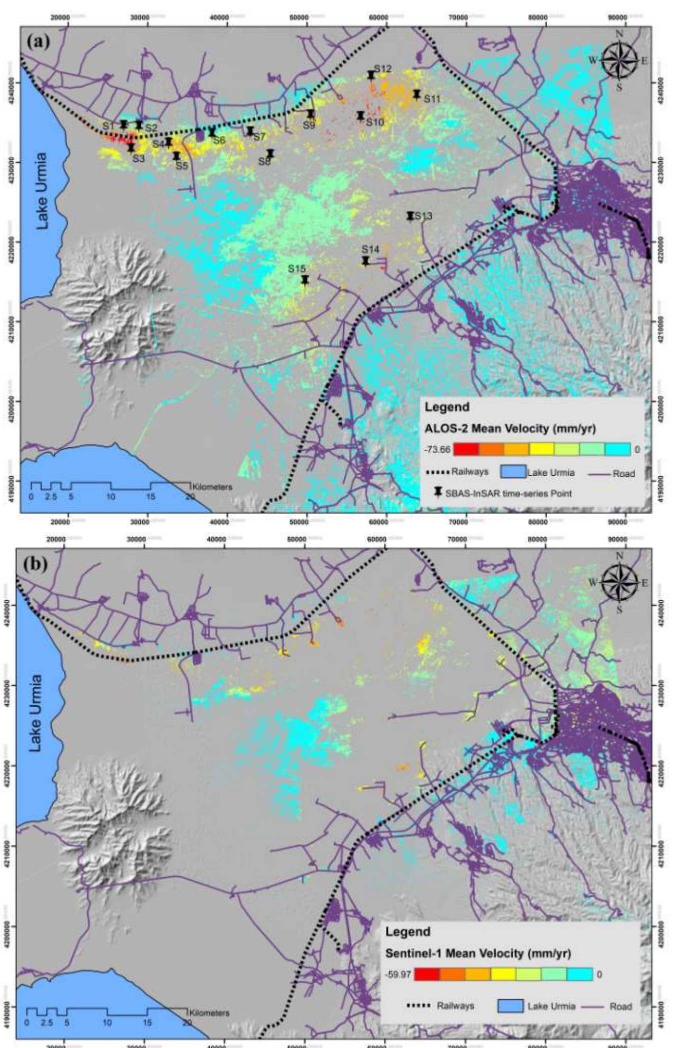

Figure 4. Mean vertical velocity maps from (a) ALOS-2 L-band (2015–2023) and (b) Sentinel-1 C-band (2017–2023).

To further evaluate the consistency and reliability of the deformation measurements obtained from the two SAR sensors, a quantitative comparison was conducted using a scatter plot between the mean deformation velocities derived from the ALOS-2 and Sentinel-1 datasets (Figure 5). The scatter plot reveals a strong linear correlation between the two datasets, indicating a high level of agreement and demonstrating the robustness of both sensors in detecting and quantifying ground subsidence across the study area. However, the deformation rates derived from ALOS-2 are slightly higher than those obtained from Sentinel-1. This difference can be attributed to the variation in temporal coverage, as the ALOS-2 dataset spans a longer observation period (2015–2023) compared to Sentinel-1 (2017–2023), thereby capturing a greater cumulative deformation signal over time.

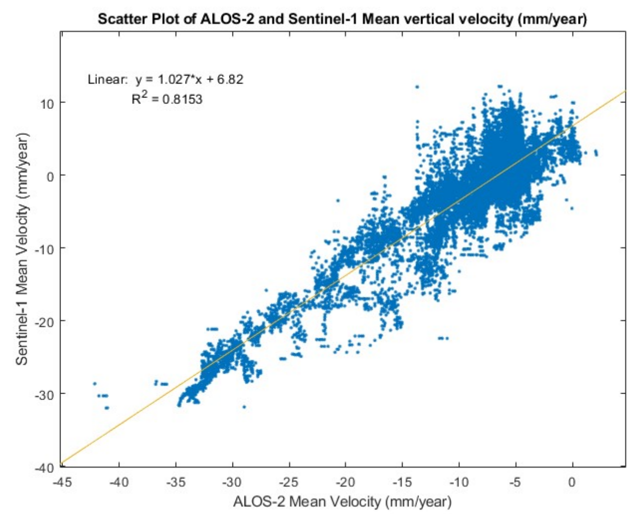

Figure 5. Scatter plot of mean vertical velocities (mm/year) derived from ALOS-2 L-band (2015–2023) and Sentinel-1 C-band (2017–2023) datasets.

Figures 6a and 6b show the time-series trends of SBAS-InSAR at 15 locations in the study area for ALOS-2 and Sentinel-1 images. These locations are shown in Figure 4a. The subsidence values at the observed locations show an increasing trend over time. To accurately analyze the time series of ground subsidence in the study area, we analyzed and compared the surface displacement data with the annual precipitation rates in the province. The precipitation data were obtained from the synoptic and rain gauge stations of East Azerbaijan Province, available through the IRDA website — the official national database for meteorological and hydrological statistics in Iran. The annual average precipitation in the study area was calculated and used for comparison with the InSAR time-series data. The annual precipitation time-series chart is shown for comparison in Figures 5a and 5b to investigate the connection between subsidence and precipitation changes. The findings show that in 2018 and 2023, increased rainfall and flooding in the region corresponded with a reduction in cumulative subsidence. Additionally, when the average precipitation showed a declining trend, the cumulative subsidence increased sharply in the region. This occurred due to increased groundwater extraction and a subsequent decline in the groundwater level.

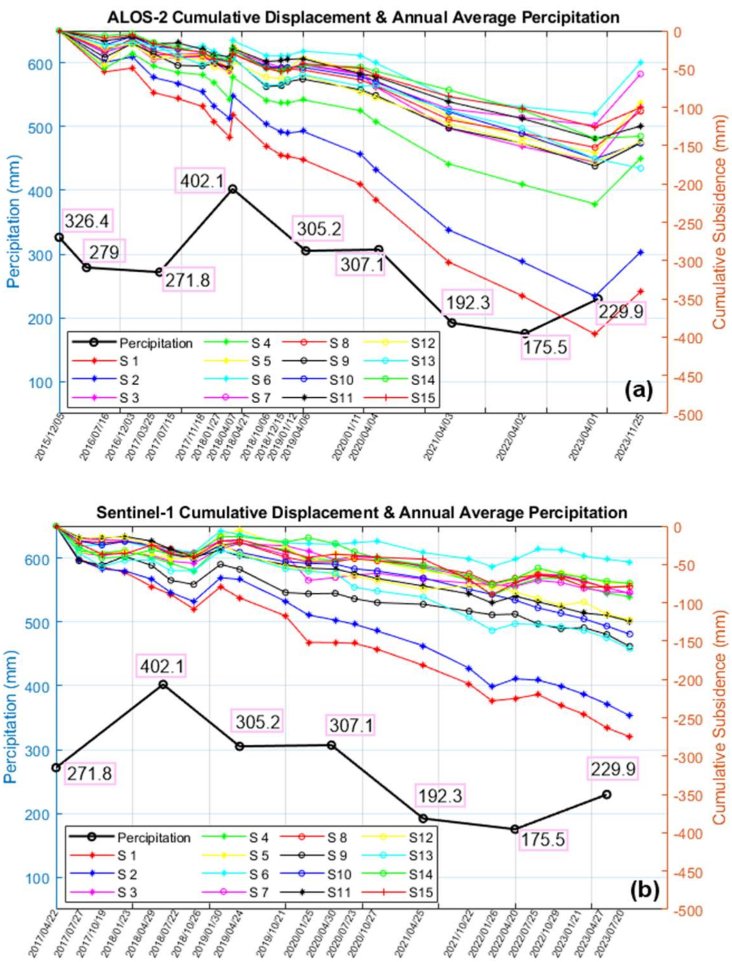

Figure 6. SBAS-InSAR time-series plots for 15 locations using (a) ALOS-2, (b) Sentinel-1, and the annual average precipitation data.

4. CONCLUSION

This study systematically analyzed ground deformation using the InSAR technique and compared the results. By integrating time-series InSAR technology with multi-sensor and multi-temporal data, ground deformation in East Azerbaijan Province, particularly in the Tabriz and Shabestar plains, was examined. In this study, two SAR datasets, ALOS-2 and Sentinel-1, were utilized to obtain time-series ground deformation in the study area from 2015 to 2023 using the SBAS-InSAR method. The findings reveal significant ground surface changes in these regions, consistent with previous studies identifying them as critical subsidence hotspots. We observed the maximum vertical subsidence rate at -73.66 mm/year for ALOS-2 and -59.97 mm/year for Sentinel-1. This discrepancy is attributed to the impact of different wavelengths and observation periods on displacement detection. Comparative analysis of ALOS-2 and Sentinel-1 data showed similar subsidence patterns, confirming the reliability of the SBAS-InSAR technique for monitoring ground surface changes. Moreover, the strong linear correlation observed between the deformation measurements of both sensors further validates their reliability. It demonstrates the high accuracy of the derived results in detecting and quantifying land subsidence. Extensive use of Sentinel-1 images can significantly improve the accuracy of SBAS analyses; however, due to the high computational requirements and time-consuming processing, only a subset of the data was used in this study. This was considered an operational limitation. In future studies, utilizing a large number of images could lead to improved accuracy of the results.

Additionally, the time-series trends indicated an overall increase in subsidence during the study period. However, in 2018 and 2023, due to increased rainfall and flooding in the area, a significant decrease in the subsidence rate was observed. This study highlights the importance of integrating remote sensing techniques with hydrological data for a better understanding of ground subsidence dynamics. Continuous monitoring using multi-source SAR data, as demonstrated in this article, can aid in identifying deformation characteristics and preventing potential damages. The results of this research provide reliable scientific evidence for developing sustainable strategies for groundwater resource management in subsidence-prone areas.

ACKNOWLEDGEMENT

The ALOS-2 images were provided by JAXA under the EO RA-3 project (ER3A2N105) for Sadra Karimzadeh.

REFERENCES

Andaryani, S., Nourani, V., Trolle, D., Dehghani, M., Asl, A. M., 2019: Assessment of land use and climate change effects on land subsidence using a hydrological model and radar technique. *Journal of Hydrology*, *578*, 124070.

Ashraf, T., Yin, F., Liu, L., Zhang, Q., 2024: Land Subsidence Detection Using SBAS-and Stacking-InSAR with Zonal Statistics and Topographic Correlations in Lakhra Coal Mines, Pakistan. *Remote Sensing*, *16*(20), 3815.

Berardino, P., Fornaro, G., Lanari, R., Sansosti, E., 2002: A new algorithm for surface deformation monitoring based on small baseline differential SAR interferograms. *IEEE Transactions on geoscience and remote sensing*, *40*(11), 2375-2383.

Haghshenas Haghighi, M., Motagh, M., 2024: Uncovering the impacts of depleting aquifers: A remote sensing analysis of land subsidence in Iran. *Science Advances*, *10*(19), eadk3039.

Huang, C., Tan, L., Liu, J., Yan, K., 2024: Multi-Temporal-InSAR Ground Deformation Mapping of Beijing Subway Network Based on ALOS-2 and Sentinel-1 Data. *Polish Journal of Environmental Studies*.

Karimzadeh, S., Matsuoka, M., 2020: Ground displacement in East Azerbaijan Province, Iran, revealed by L-band and C-band InSAR analyses. *Sensors*, *20*(23), 6913.

Karimzadeh, S., Zulfikar, A. C., Matsuoka, M., 2024: Time series analysis of L-band PALSAR-2 images in Istanbul and Kocaeli, Turkey. *Big Earth Data*, 1-27.

Sorkhabi, O. M., Khajehzadeh, M., Keawsawasvong, S., 2023: Landslides monitoring with SBAS-InSAR and GNSS. *Physics and Chemistry of the Earth, Parts A/B/C*, *132*, 103486.

Su, Z., Wang, E. C., Hu, J. C., Talebian, M., Karimzadeh, S., 2016: Quantifying the termination mechanism along the North Tabriz-North Mishu Fault Zone of Northwestern Iran via small baseline PS-InSAR and GPS decomposition. *IEEE Journal of selected topics in applied Earth observations and remote sensing*, *10*(1), 130-144.

Yi, X., Wang, L., Ci, H., Wang, R., Yang, H., Yan, Z., 2025: Monitoring of Land Subsidence and Analysis of Impact Factors in the Tianshan North Slope Urban Agglomeration. *Land*, *14*(1), 202.

Zhang, J., Kou, P., Tao, Y., Jin, Z., Huang, Y., Cui, J., Liu, R., 2024: Urban ground subsidence monitoring and prediction using time-series InSAR and machine learning approaches: a case study of Tianjin, China. *Environmental Earth Sciences*, *83*(16), 473.